Reaction Forces Developed on Specially Reinforced Anti Collapse Steel Beam to Tubular Column Connection Under Dynamic Loading

Anurag Sanjay Deshmukh[1], Prof. P. S. Lande[2]
[1]*M.Tech Student, Department of Applied Mechanics, Government College of Engineering, Amravati, Maharashtra, India*
[2]*Associate Professor, Department of Applied Mechanics, Government College of Engineering, Amravati, Maharashtra, India*

***Abstract*: In steel structures, connections can be made to reduce the likelihood of progressive collapse in particular situations. The impacts are examined in this research using a specifically strengthened beam to tubular column connection that has previously been subjected to monotonic loading analysis. Due to the fact that every structure is primarily intended for static loading, dynamic loading is a key challenge. That isn't actually conceivable because static and normal loads will always act. Therefore, the primary goal of this study is to validate the modal similar connection in the ABAQUS software that is described in the base work and to investigate all behavioral patterns of failure of beam column joints under column removal technique. The link has undergone a finite element analysis. Although all other parameters are maintained from the previous study, the link is tested for dynamic loading up until failure. D'alembert's principal is used to compute dynamic loading before static loading in order to achieve the purpose. The connection is affected by the calculated amplitude in the case of a column removal. Numerous possibilities are addressed in the study since unexpected events can lead to progressive breakdown. Results for reaction load and displacement are displayed graphically. The graphical interpretation is finished after that. Calculated and contrasted with static loading are catenary and flexural actions.**

***Index Terms:* D'alembert's principal, Dynamic Loading, Progressive Collapse.**

I. INTRODUCTION

The problems that affect strengthening and retrofitting strategies are not well understood or even thoroughly discussed. The vast majority of the currently available published work focuses on the redistribution-type collapse in single member loss scenarios, such as static or dynamic column removal, either explicitly or implicitly. Only specific sorts of standard cases often respond favorably to the suggested strengthening and retrofitting techniques. The procedures that prevent collapse can differ based on the structural systems and initial damage regimes, according to numerous recent research. In general, catenary action and flexural action play a significant role in transferring loads to neighboring columns. In this regard, this part provides a summary of the factors that influence the strengthening and retrofitting strategy. If we take the effect of Progressive collapse into account when developing any link, we must take all the parameters into account. Such as structural topology, initial failure type and severity, and collapse typology impacts.

Test Specimen: As seen in Figures 1 and 2, when the components of the joint were linked, the specimen's bottom flange was strengthened with a cover plate using M24 common bolts (Grade-10.9 high-strength bolts without applying pre-tension, similar to ASTM A490 bolts). The specimens' geometrical characteristics are listed in Figure 2. Grade Q345 steel was used for all beams, columns, through diaphragms, shear tabs, and cover plates, same like with ASTM A572 Grade 50. The material specifications for each component, as established by three coupon tests, are listed in Table 1.

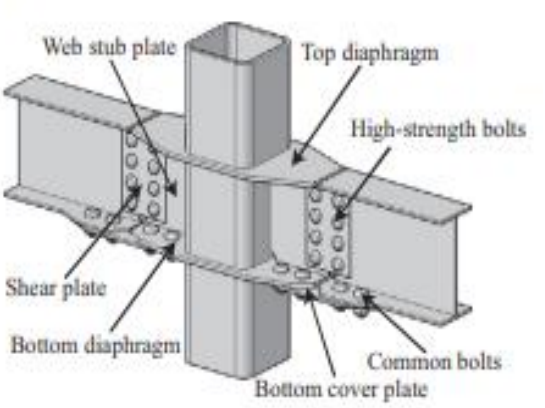

Figure 1: Specimen Assembly [1]

The span of the beam, which is l0 (4500 mm), represents the separation between the inflection points. The main column has a height of 900 mm. Designing the beams and columns in accordance with Chinese codes led to the adoption of H300x150x6x8 mm and RHS 250x14 mm sections, respectively. Each specimen had two diaphragms placed within it through the column, at the top and bottom flanges of the beam. Shear tabs and cover plates are 8 mm (corresponding to the thickness of the beam flange) and 6 mm (similar to the thickness of the beam web), respectively, thick in accordance with the equal bearing capacity principle. Diaphragms are 4 mm thicker than the 12 mm thick beam flanges.

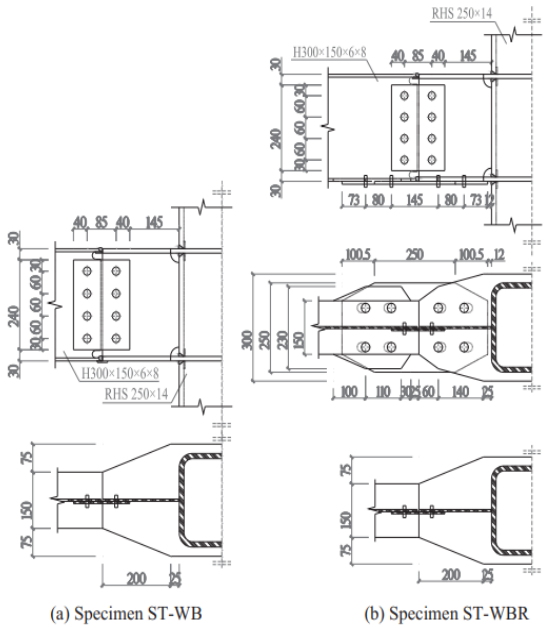

Figure 2: Details of Specimen [1]

Each beam web and its accompanying web stub plate were attached to the shear tab using four M20 Grade-10.9 slip-critical high-strength bolts applied with a pretension of 155 kN, which are comparable to high-strength bolts in accordance with ASTM A490. The four bolts are capable of transmitting the complete shear force produced by the beam web. The 200 mm long transition zone of the diaphragms provides sufficient space for cover plates and high tensile strength bolts. All of the contact surfaces were cleaned using sandblasting.

Table 1: Material Properties

Components	Fy (MPa)	Fu (MPa)	δ (%)	(σ1)	(Ɛ1)
RHS (250X250)	482	545	24	739	1.134
Beam Flange (8mm)	387	441	31	661	0.665
Beam Web (t = 8mm)	417	514	27	796	0.731
Diaphragm (t = 12mm)	450	574	24	915	0.627

Finite Element Analysis: In order to perform analytical tests, precise non-linear static finite element (FE) models were built in ABAQUS finite element analysis software using the "explicit dynamic" analysis approach, which is suitable for complex contact scenarios like those in precast connections. The influence of loads and abrupt column removal were evaluated on the models. In the sections that follow, the developed models are detailed in detail along with a comparison of the predicted responses' accuracy to the results of the experimental testing. For better numerical performance, solid type C3D8R elements with 8 nodes and reduced integration were specified for the structural members and connecting components. There were four layers of solid elements on each plate, resulting in an element thickness ranging from 1.5 to 3.5 mm. The solid components had dimensions of 2 mm in the connection zone and 2–20 mm outside of it. Contact with friction was detailed between the bolts, beam flanges, beam webs, shear tabs, web stub plates, diaphragms, and cover plates in order to model the transmission of forces through the bolted connection. The specimen's FE mesh and the world's Cartesian coordinates are shown in Figure 3. The boundary and loading conditions of the model are also shown in Figure 3.

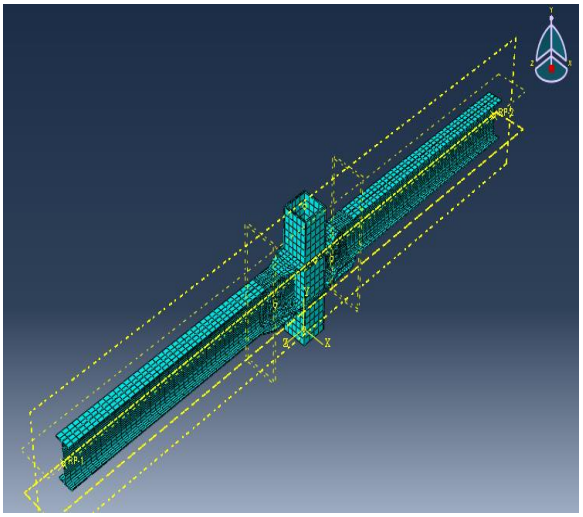

Figure 3: Beam Column connection with 25mm meshing

At the ends of the beams, rotations and displacements in all planes were restricted to mimic the pin supports. To guarantee a static response, displacements on the center column stub were slowly increased. The FE model took into account the issue with the welding between the west beam flange and the reinforcing plate. In particular, the beam flange was not integrated with half of the reinforcing plate in the thickness direction. There will be some discrepancies between the test findings and the finite element results since the FE simulation cannot account for some issues, such as material defects and installation mistakes.

II. ASSEMBLY

A square column is positioned in the middle of the assembly, with the top and bottom diaphragms spaced 276 mm apart, fixed by welding, and represented by a tie constraint in the finite element model using the surface-to-surface discretization method. Web stud between the two diaphragms with a tie constraint in FEM and a surface-to-surface discretization technique. Beam and top diaphragm are tied together in the FEM using the surface-to-surface discretization approach. Shear plates are attached to beam web and web stands using M20 grade bolt plates with a 155KN pretension. M24 grade 16mm and M24 grade 20mm shank bolts are used to attach the bottom cover plate to the flange and the bottom diaphragm, respectively.

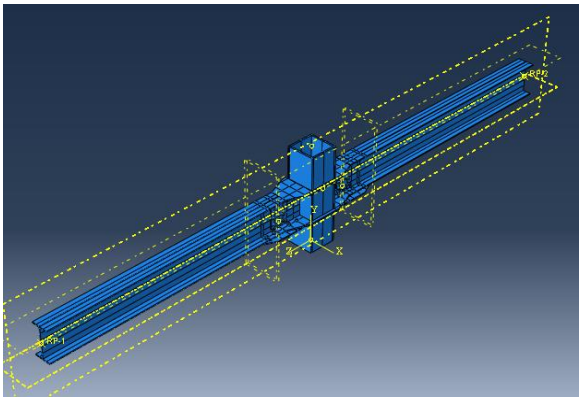

Figure 4: Beam to Column Assembly

III. LOADING CALCULATION

D'Alemberts Principle: This approach is straight forward and treats dynamic in a direct manner by always relating external force to the acceleration. Considering body of mass 'm' attach to spring whose stiffness is 'k' by external force 'p' body is pulled away to a distance x0 which is initial amplitude. At time t=0 the force 'p' is removed, the body is in state of free vibration. To bring the body to a state of artificial equilibrium known as Dynamic equilibrium, all that we need to do is to add the inertia force mx¨. In the direction opposite to the direction of motion in accordance to the D'Alemberts Principle.

Applying equilibrium condition ∑〖fx=0〗

When t=0, dx/dt=x ̇0

Now, x = a=A sin pt

dy/dt=A p cospt

x = A cos pt + B sin pt

Where A and B are arbitrary constants

dx/dt=x ̇ = -Ap sin pt + Bp cos pt

(d^2 x)/〖dt〗^2 =x ̈= -Ap2 cos pt + Bp2 sin pt

Putting boundary conditions:

t=0, x=x0, x ̇=v0

x0= A×1+B×0

A=x0

V0= -A×p×0+B×p×1

V0=B×p

B=V0/p

So, general solution becomes,

$x = x0 \times \cos pt + (V0/p) \times \sin pt$

$x = \sqrt{(\ [x0]\ ^2 + [(V0/p)]\ ^2\ )} \times \sin (pt + \propto 2\ )$

Where, $\propto 2 = \tan^{-1}(x0/((V0/p)))$

$x = \sqrt{(\ [x0]\ ^2 + [(V0/p)]\ ^2\ )} \times \cos (pt + \propto 1\ )$

where, $\propto 1 = \tan^{-1}(((V0/p))/x0)$

This indicates that amplitude of vibration

Amplitude $= \sqrt{(\ [x0]\ ^2 + [(V0/p)]\ ^2\ )}$

$p = \sqrt{(k/m)}$

$\tau = 2\pi/p$

$f = 1/\tau$ cps

As shown in above derivation of D'alembert's principal Time Period and Amplitude is calculated listed in table 2 and graphically represented in figure 5 in incremental form.

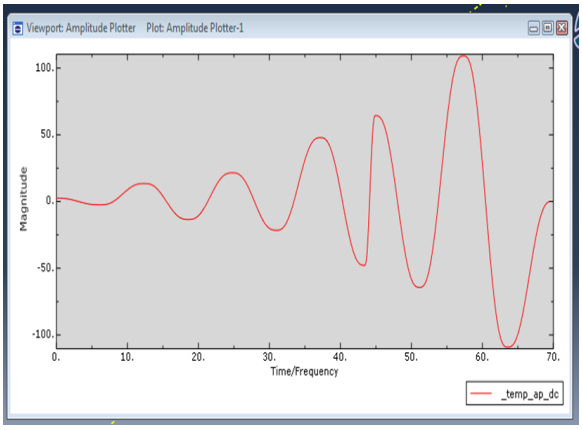

Figure 5: Time Vs Amplitude

Table 2: Calculated Amplitude

Time Period	Amplitude
0	2.5
6.2	-2.5
12.4	13.474
18.6	-13.474
24.8	21.515
31	-21.515
37.2	47.883
43.4	-47.883
44.95	64.39
51.15	-64.39
57.35	109.2
63.55	-109.2
69.75	0

IV. RESULTS

4.1 Hysteresis Behaviour: It is shown in hysteresis curve figure 6 the downward load is defined as positive load and upward load is defined as negative load whereas negative displacement defined as downward displacement and positive displacement defined as upward displacement visualized in figure 7.

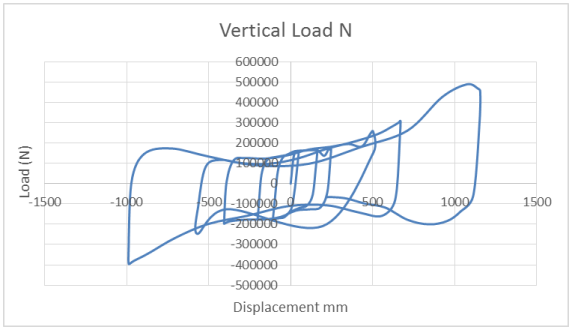

Figure 6: Hysteresis Curve

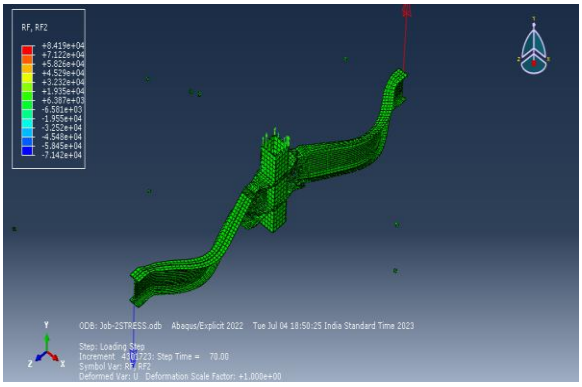

Figure 7: Visualization of Vertical Forces

Vertical Load Resisted:- From figure 4.4 maximum load reached in positive and negative direction are given in table 3.

Table 3: Reaction Force Development

Displacement mm	Vertical Load KN
47.2603	161.602
39.5273	79.1671
-107.493	-173.350
-96.6862	-78.2541
163.123	166.037
154.276	87.6396
-177.562	-175.938
-196.08	-120.621
231.956	170.146
243.147	132.218
-406.302	-197.143
-405.567	-179.658
502.811	256.463

-569.512	-246.954
-561.106	-94.6541
669.72	308.187
667.344	252.085
-987.347	-396.223
-989.576	-368.081
1074.37	489.204
1152.11	309.715

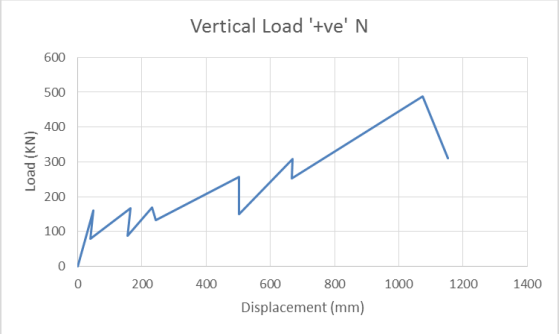

Figure 8: Vertical Load '+ve'

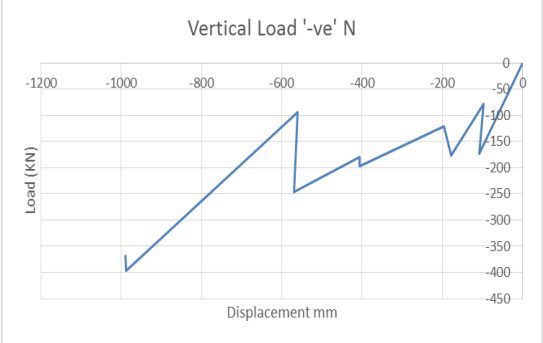

Figure 9: Vertical Load '-ve'

From table 3 and figure 8 and 9 following results are interpreted. In figure 8 and 9 each increment line shows one cycle of amplitude loading.

1] With displacement changes from 47.26 mm to 39.52 mm in the positive direction, the load in the first cycle increased to a maximum of 161.815 KN and then decreased to 79.167 KN. In contrast, over the same cycle, the load increased to -173.35 KN and decreased to -78.254 KN with changes in displacement from -107.86 mm to -96.68 mm.

2] In the second cycle, load increased to 166.037 KN and decreased to 87.63 KN while displacement changed in a positive manner from 163.123 mm to 154.27 mm. While in the same cycle, the load fluctuated between -175.938 KN and -120.621 KN with a change in displacement from -177.562 mm to -196.08 mm.

3] In the third cycle, the load increased to 170.146 KN and then decreased to 132.118 KN, with displacement changes in the positive direction from 231.95 mm to 243.147 mm. In contrast, over the same cycle, the load fluctuated between -197.143 KN and -179.658 KN with a change in displacement from -406.30 mm to -405.56 mm.

4] In the fourth cycle, the load increased to 256.463 KN and decreased to 149.244 KN, with positive displacement changes from 502.81 mm to 502.425 mm. However, over the same cycle, the load fluctuated between -246.95 KN and -94.65 KN with a change in displacement from -569.51 mm to -561.10 mm.

5] In the fifth cycle, the load increased to 308.187 KN and then decreased to 252.08 KN, with displacement moving in a positive direction from 669.72 mm to 667.34 mm. However, during the same cycle, the load increased to -396.223 KN and then decreased to -368.081 KN with changes in displacement from -987.34 mm to -989.57 mm.

6] In the sixth cycle, the load increased to 489.20 KN and then decreased to 309.715 KN, with positive displacement variations from 1074.37 mm to 1152.11 mm. While in the same cycle, the load fluctuated between 396.223 KN and 368.081 KN with a change in displacement from 987.34 mm to 989.57 mm.

V. CONCLUSION

1] In this study, the dynamic analyses of a specifically reinforced beam column joint used to prevent collapse are compared. Following results are drawn after a successful analysis of the behavior of the steel beam column connection using various parameters.

2] Reaction Forces developed in positive direction and negative direction are approximately same but in negative direction reaction force is less than positive direction.

3] This is because when loading is applied on connection firstly it goes in downward direction which is positive where joint loses its small amount of stiffness.

REFERENCES

1] A special reinforcing technique to improve resistance of beam-to-tubular column connections for progressive collapse prevention Xi Qin a,b , Wei Wang a,b,⇑ , Yiyi Chen a,b , Yihai Bao c a State Key

Laboratory of Disaster Reduction in Civil Engineering, Tongji University, Shanghai 200092, China bDepartment of Structural Engineering, Tongji University, Shanghai 200092, China cDepartment of Civil and Environmental Engineering, University of California-Davis, Davis, CA 95616, USA

2] Experimental Investigation of Beam–Column Joints with Cast Steel Stiffeners for Progressive Collapse Prevention Qinghua Han, Ph.D.1 ; Xinxia Li2 ; Mingjie Liu, Ph.D.3 ; and Billie F. Spencer Jr., Ph.D., F.ASCE

3] Progressive collapse behavior of joints in steel moment frames involving reduced beam section Canwen Chen a , Huiyun Qiao b , Jinpeng Wang a , Yu Chen a,* a College of Civil Engineering, Fuzhou University, Fuzhou 350116, China b College of Civil Engineering, Fujian University of Technology, Fuzhou 350118, China

4] Experimental and numerical investigation on the anti-progressive collapse performance of fabricated connection with CFST column and composite beam Long Zheng a , Wen-Da Wang a,b,* , Wei Xian a,b a School of Civil Engineering, Lanzhou University of Technology, Lanzhou 730050, PR. China b Western Center of Disaster Mitigation in Civil Engineering of Ministry of Education, Lanzhou 730050, PR. China

5] Progressive Collapse Analysis of Concrete-filled Steel Tubular Column to Steel Beam Connections Using Multi-scale Model Wenda Wang ∗, Huawei Li, Jingxuan Wang The Key Laboratory of Disaster Prevention and Mitigation in Civil Engineering of Gansu Province, Lanzhou University of Technology, Lanzhou, Gansu Province, China

6] Anti-collapse performance assessment of steel beam-column substructures with all-welded connections after exposure to fire Zhan Guo a, Zhiquan Xing a , Heng Zhang a , Hanwu Zhang b , Long Chen c , Yu Chen a,* a College of Civil Engineering, Fuzhou University, Fuzhou 350116, China b Fujian yongdongnan Construction Group Co., Ltd, Fuzhou 350700, China c Fujian jintong Construction Group Co., Ltd, Fuzhou 350300, China

7] Strengthening and retrofitting techniques to mitigate progressive collapse: A critical review and future research agenda Foad Kiakojouri a,b , Valerio De Biagi a,b,∗ , Bernardino Chiaia a,b , Mohammad Reza Sheidaii c a Department of Structural, Geotechnical and Building Engineering (DISEG) - Politecnico di Torino, Torino, Italy b SISCON-Safety of Infrastructures and Constructions, Politecnico di Torino, Torino, Italy c Department of Civil Engineering, Urmia University, Urmia, Iran

8] Numerical study on the anti-progressive collapse performance of steel frame-steel plate shear wall structures Bao Meng a,b , Jiping Hao a,b,* , Weihui Zhong a,b a Department School of Civil Engineering, Xi'an University of Architecture & Technology, Xi'an, 710055, China b Key Lab of Structural Engineering and Earthquake Resistance, Ministry of Education (XAUAT), Xi'an, 710055, China

9] Design of Building to resist progressive collapse, UFC 4-023-03

10] Acceptance criteria for moment frames based on structural testing and commentary, ACI 374.1-05

11] Improvement of nonlinear static seismic analysis procedure, FEMA440,(2005), Applied Technology Council Redwood shores parkway suit 240